AFRL-AFOSR-VA-TR-2019-0010

Studies and Computer Codes for Currents, Fields and Plasmas in the Turbulent Upward and Downward Current Systems of the Earth's Magnetosphere

John Jasperse
BOSTON COLLEGE CHESTNUT HILL MA

01/04/2019
Final Report

Air Force Research Laboratory
AF Office Of Scientific Research (AFOSR)/ RTB1
Arlington, Virginia 22203
Air Force Materiel Command

DISTRIBUTION A: Distribution approved for public release.

REPORT DOCUMENTATION PAGE

Form Approved
OMB No. 0704-0188

1. REPORT DATE *(DD-MM-YYYY)*	2. REPORT TYPE	3. DATES COVERED *(From - To)*
04-01-2019	Final Performance	30 Sep 2015 to 29 Sep 2018

4. TITLE AND SUBTITLE
Studies and Computer Codes for Currents, Fields and Plasmas in the Turbulent Upward and Downward Current Systems of the Earth's Magnetosphere

5a. CONTRACT NUMBER

5b. GRANT NUMBER
FA9550-15-1-0475

5c. PROGRAM ELEMENT NUMBER
61102F

6. AUTHOR(S)
John Jasperse, Bamandas Basu, Eric Lund, Neil Grossbard

5d. PROJECT NUMBER

5e. TASK NUMBER

5f. WORK UNIT NUMBER

7. PERFORMING ORGANIZATION NAME(S) AND ADDRESS(ES)
BOSTON COLLEGE CHESTNUT HILL MA
140 COMMONWEALTH AVE
CHESTNUT HILL, MA 02467-3853 US

8. PERFORMING ORGANIZATION REPORT NUMBER

9. SPONSORING/MONITORING AGENCY NAME(S) AND ADDRESS(ES)
AF Office of Scientific Research
875 N. Randolph St. Room 3112
Arlington, VA 22203

10. SPONSOR/MONITOR'S ACRONYM(S)
AFRL/AFOSR RTB1

11. SPONSOR/MONITOR'S REPORT NUMBER(S)
AFRL-AFOSR-VA-TR-2019-0010

12. DISTRIBUTION/AVAILABILITY STATEMENT
A DISTRIBUTION UNLIMITED: PB Public Release

13. SUPPLEMENTARY NOTES

14. ABSTRACT
In this work, we carried out studies of satellite and ground-based data and performed basic research on the currents, fields, and plasmas in the upward and downward current systems of the Earth's magnetosphere when turbulence is present and when turbulence is neglected or absent. In this way, we seek to improve the capability of the Air Force (AF) to specify and predict the state of the plasma in the coupled magnetosphere-ionosphere (M-I) system. It is well known that perturbations of the near-Earth space environment can disrupt important AF systems and thereby interfere with global command, control, communication, intelligence, surveillance, and reconnaissance procedures. Based on our studies, we developed four models and computer codes based on these models. The models describe the intermediate temporal and spatial evolution of the upward and downward Birkeland currents when turbulence is present and when turbulence is neglected or absent. We have documented and will provide the computer codes to the AF and other scientific users upon request.

15. SUBJECT TERMS
Aurora, Birkeland Currents

16. SECURITY CLASSIFICATION OF:			17. LIMITATION OF ABSTRACT	18. NUMBER OF PAGES	19a. NAME OF RESPONSIBLE PERSON
a. REPORT	b. ABSTRACT	c. THIS PAGE			MOSES, JULIE
Unclassified	Unclassified	Unclassified	UU		19b. TELEPHONE NUMBER *(Include area code)* 703-696-9586

Standard Form 298 (Rev. 8/98)
Prescribed by ANSI Std. Z39.18

FINAL PERFORMANCE REPORT

1. Cover Sheet

AFOSR Grant Number	**FA9550-15-1-0475**
Descriptive Title	**Studies and Computer Codes for Currents, Fields, and Plasmas in the Turbulent Upward and Downward Current Systems of the Earth's Magnetosphere**
Principal Investigator	**Dr. John R. Jasperse**
Institution	**Institute for Scientific Research** **Boston College** **140 Commonwealth Av., 02467**
Commercial Phone	**617 552 6368**
E-Mail Address	**john.jasperse@bc.edu**
AFOSR Program Manager	**Dr. Julie Moses**
E-Mail Address	**julie.moses@us.af.mil**
Reporting Period	**September 29, 2015 to September 29, 2018**

2. Objectives

In this work, we carried out studies of satellite and ground-based data and performed basic research on the currents, fields, and plasmas in the upward and downward current systems of the Earth's magnetosphere when turbulence is present and when turbulence is neglected or absent. In this way, we seek to improve the capability of the Air Force (AF) to specify and predict the state of the plasma in the coupled magnetosphere-ionosphere (M-I) system. It is well known that perturbations of the near-Earth space environment can disrupt important AF systems and thereby interfere with global command, control, communication, intelligence, surveillance, and reconnaissance procedures. Based on our studies, we developed four models and computer codes based on these models. The models describe the intermediate temporal and spatial evolution of the upward and downward Birkeland currents when turbulence is present and when turbulence is neglected or absent. We have documented and will provide the computer codes to the AF and other scientific users upon request.

3. Status of Effort

In sections 5 and 6 of the AFOSR Proposal, we gave the results to be achieved in years 1, 2, and 3. We have developed the four computer codes in the three years of the proposed work. We developed codes 1 and 3 in the first year and codes 2 and 4 in the second and third years. See section 6 of the AFOSR proposal. For a discussion of codes 2 and 4 see section 4 of this Final Report.

4. Research Accomplishments

4.1 The Multiconstituent, Multimoment Fluid Equations for the Turbulent Birkeland Current System.

4.1.1 The multiconstituent, multimoment fluid equations in the guiding-center and gyrotropic approximation for weak electrostatic turbulence.

The ensemble-averaged Vlasov-Maxwell equations for weak electrostatic turbulence may be determined by neglecting $\delta\mathbf{B}$ but retaining $\delta\mathbf{E}$ in the expressions for the wave-particle correlation functions for the problem, and by choosing a time-independent model for $\langle\mathbf{B}\rangle$: $\delta\mathbf{B}\to 0, \langle\mathbf{B}\rangle = \mathbf{B}(\mathbf{r})$. Here, the symbol $\langle\ \rangle$ denotes the ensemble average of a quantity, $\delta\mathbf{E}$ and $\delta\mathbf{B}$ are the time-dependent fluctuations of the electric and magnetic fields, respectively, and $\delta\mathbf{B}$ is set to zero, since only electrostatic turbulence is considered in this section.

This yields the ensemble-averaged Vlasov-Maxwell equations for electrostatic turbulence given by

$$\left\{\frac{\partial}{\partial t}+\mathbf{v}\cdot\frac{\partial}{\partial\mathbf{r}}+\frac{q_\alpha}{m_\alpha}\left[\langle\mathbf{E}\rangle+\frac{1}{c}\mathbf{v}\times\mathbf{B}\right]\cdot\frac{\partial}{\partial\mathbf{v}}\right\}\langle \mathrm{f}_\alpha\rangle = \mathrm{C}_\alpha, \tag{1}$$

$$\mathrm{C}_\alpha = -\frac{q_\alpha}{m_\alpha}\left\langle\delta\mathbf{E}\cdot\frac{\partial}{\partial\mathbf{v}}\delta \mathrm{f}_\alpha\right\rangle, \tag{2}$$

$$\frac{\partial}{\partial \mathbf{r}}.\langle \mathbf{E} \rangle = 4\pi\rho\,, \qquad \frac{\partial}{\partial \mathbf{r}} \times \langle \mathbf{E} \rangle = 0. \tag{3}$$

Here, we can write $\langle \mathbf{E} \rangle = -\left(\partial\phi / \partial \mathbf{r}\right)$, so we obtain Poisson's equation

$$\frac{\partial^2}{\partial \mathbf{r}^2}\phi = -4\pi\rho. \tag{4}$$

These equations are given in Gaussian units and are valid in the standard six-dimensional phase space. The quantities denoted here have their standard definitions.

In the guiding-center and gyrotropic approximation, we find that the kinetic equations can be simplified and are

$$\left\{\frac{\partial}{\partial t} + \mathrm{v}_{\parallel}\frac{\partial}{\partial s} + \frac{q_\alpha}{m_\alpha}\mathrm{E}_{\parallel}\frac{\partial}{\partial \mathrm{v}_{\parallel}} - \frac{1}{2B}\frac{dB}{ds}\left[\mathrm{v}_{\perp}^2\frac{\partial}{\partial \mathrm{v}_{\parallel}} - \mathrm{v}_{\parallel}\mathrm{v}_{\perp}\frac{\partial}{\partial \mathrm{v}_{\perp}}\right]\right\}\bar{\mathrm{f}}_\alpha = \overline{\mathrm{C}}_\alpha\,, \tag{5}$$

$$\bar{\mathrm{f}}_\alpha = \bar{\mathrm{f}}_\alpha\left(s,t,\mathrm{v}_{\perp},\mathrm{v}_{\parallel}\right) = \left(2\pi\right)^{-1}\int_0^{2\pi} d\varphi\langle \mathrm{f}_\alpha \rangle, \tag{6}$$

$$\overline{\mathrm{C}}_\alpha = \overline{\mathrm{C}}_\alpha\left(s,t,\mathrm{v}_{\perp},\mathrm{v}_{\parallel}\right) = \left(2\pi\right)^{-1}\int_0^{2\pi} d\varphi \mathrm{C}_\alpha\,, \tag{7}$$

where s denotes the distance along **B** and φ is the gyrophase angle, both of which are expressed in the guiding-center coordinate system. The bar symbol denotes the gyrophase average which is also calculated in the guiding-center coordinate system. The guiding-center coordinate system is one where the velocity-space coordinates slowly change their orientation as s varies so that the v_z axis is always parallel to **B**. In general, the **B** field is curved and varies slowly in space as described above. We interpret $\bar{\mathrm{f}}_\alpha\left(s,t,\mathrm{v}_{\perp},\mathrm{v}_{\parallel}\right)ds\mathrm{v}_{\perp}d\mathrm{v}_{\perp}d\mathrm{v}_{\parallel}$ as $\left(2\pi\right)^{-1}$ times the average number of particles per unit area of type α for which the coordinates of the guiding center of the motion lie between s and $s+ds$ while the velocities, $\mathrm{v}_{\perp}$ and $\mathrm{v}_{\parallel}$, lie between $\mathrm{v}_{\perp}$ and $\mathrm{v}_{\perp}+d\mathrm{v}_{\perp}$ and $\mathrm{v}_{\parallel}$ and $\mathrm{v}_{\parallel}+d\mathrm{v}_{\parallel}$, respectively. Poisson's equation becomes

$$\partial^2\phi / \partial s^2 = -4\pi\rho, \tag{8}$$

where $\phi = \phi\left(s,t\right)$ and

$$\rho = \rho\left(s,t\right) = \sum_\alpha q_\alpha \int d^3\mathrm{v}\bar{\mathrm{f}}_\alpha\left(s,t,\mathrm{v}_{\perp},\mathrm{v}_{\parallel}\right). \tag{9}$$

Here, $\bar{\mathrm{f}}_\alpha$ is normalized so that $\int d^3\mathrm{v}\bar{\mathrm{f}}_\alpha = n_\alpha$, where n_α is the number density and $\langle \mathrm{E}_{\parallel} \rangle = \mathrm{E}_{\parallel} = -\partial\phi / \partial s$.

When the model for **B** is specified and when $\overline{\mathrm{C}}_\alpha$ is given, then (5) and (7) are the system of kinetic equations in the guiding-center and gyrotropic approximation that describe the problem, subject to appropriate initial-value and/or boundary-value conditions. When $dB/ds \neq 0$, a direct numerical solution or some orthonormal expansion method of solving (5) and (7) can be

considered. For a uniform **B** field, $dB/ds = 0$, and the left-hand side of (5) does not contain $\mathrm{v}_\perp$, but the right-hand side does. For this case, we note that an orthonormal expansion method on the $\mathrm{v}_\perp$ variable needs to be considered. However, in the remainder of report, we pursue the multiconstituent, multimoment fluid equations as a method of solution for the problem.

We now assume that the fluctuating electric field is random (Markovian), that the length and time scales for the one-particle distribution functions and the two-particle correlation functions separate, and that C_α is given by a velocity-space Fokker-Planck operator

$$\mathrm{C}_\alpha = -\frac{\partial}{\partial \mathbf{v}} \cdot \left(\mathbf{F}_\alpha^f + \mathbf{F}_\alpha^p \right) \mathrm{f}_\alpha + \frac{1}{2} \frac{\partial}{\partial \mathbf{v}} \frac{\partial}{\partial \mathbf{v}} : \mathbf{D}_\alpha^f \mathrm{f}_\alpha, \tag{10}$$

where $\mathbf{F}_\alpha^f$, $\mathbf{F}_\alpha^p$, and $\mathbf{D}_\alpha^f$ are functionals of $\tilde{\varepsilon}$ and $\left\langle \left| \delta E^2 \right| \right\rangle$, and where $\tilde{\varepsilon}$ and $\left\langle \left| \delta E^2 \right| \right\rangle$ are the dielectric screening function and spectral density of the longitudinal electric-field fluctuations for the turbulent plasma, respectively. By separation of length and time scales, we mean that there is a length l and time τ such that $l_1 >> l >> l_2 \sim \lambda_{De}$ and $\tau_1 >> \tau >> \tau_2 \sim \omega_{pe}^{-1}$, where λ_{De} is the electron Debye length and ω_{pe} is the electron plasma frequency. Here, l_1 and τ_1 are the characteristic length and time scales for the one-particle distribution functions, respectively. In the guiding-center and gyrotropic approximation, we consider a Cartesian, velocity-space coordinate system which slowly changes its orientation as *s* varies along **B** so that the v_z axis is always parallel to **B.** Thus, $\mathrm{v}_\parallel^2 = \mathrm{v}_\mathrm{z}^2$ and $\mathrm{v}_\perp^2 = \mathrm{v}_\mathrm{x}^2 + \mathrm{v}_\mathrm{y}^2$.

We now calculate the multiconstituent, multimoment fluid equations in the guiding-center and gyrotropic approximation by taking the velocity moments of equations (5)-(7). We obtain:

$$\frac{\partial}{\partial t} n_\alpha + B \frac{\partial}{\partial s} \left(n_\alpha u_\alpha / B \right) = 0, \tag{11}$$

$$\frac{\partial}{\partial t} m_\alpha n_\alpha u_\alpha + \frac{\partial}{\partial s} n_\alpha \left(T_{\alpha\parallel} + m_\alpha u_\alpha^2 \right) - \frac{1}{B} \frac{dB}{ds} n_\alpha \left(T_{\alpha\parallel} + m_\alpha u_\alpha^2 - T_{\alpha\perp} \right) + q_\alpha n_\alpha \frac{\partial \phi}{\partial s} = \dot{M}_{\alpha\parallel}, \tag{12}$$

$$\frac{1}{2} \frac{\partial}{\partial t} n_\alpha \left(T_{\alpha\parallel} + m_\alpha u_\alpha^2 \right) + \frac{\partial}{\partial s} n_\alpha q_{\alpha\parallel} - \frac{1}{B} \frac{\partial B}{\partial s} n_\alpha \left(q_{\alpha\parallel} - q_{\alpha\perp} \right) + q_\alpha n_\alpha u_\alpha \frac{\partial \phi}{\partial s} = \dot{W}_{\alpha\parallel}, \tag{13}$$

$$\frac{\partial}{\partial t} n_\alpha T_{\alpha\perp} + B^2 \frac{\partial}{\partial s} \left(n_\alpha q_{\alpha\perp} / B^2 \right) = \dot{W}_{\alpha\perp}, \tag{14}$$

$$\frac{\partial^2 \phi}{\partial s^2} = -4\pi \sum_\beta q_\beta n_\beta. \tag{15}$$

Here, (11)-(15) are a set of $4N+1$ equations for the $6N+1$ unknowns: n_α, u_α, $T_{\alpha\parallel}$, $T_{\alpha\perp}$, $q_{\alpha\parallel}$, $q_{\alpha\perp}$, and ϕ. N is the number of plasma constituents. Here, n_α is the number density, u_α is the drift velocity parallel to **B**, $T_{\alpha\parallel}$ is the parallel temperature, $T_{\alpha\perp}$ is the perpendicular temperature, $q_{\alpha\parallel}$ is the total parallel energy-flux per particle, and $q_{\alpha\perp}$ is the total perpendicular energy-flux per particle. Also, ϕ is the electrostatic potential, $g_\parallel$ is the gravitational acceleration either

parallel or antiparallel to **B,** B is the geomagnetic field strength, *s* is the distance along **B,** and the other quantities have their usual meanings.

The anomalous transfer-rates per unit volume due to turbulent wave-particle interactions denoted by $\dot{M}_{\alpha\|}, \dot{W}_{\alpha\|}$ and $\dot{W}_{\alpha\perp}$ in (12) - (14) are

$$\begin{bmatrix} \dot{M}_{\alpha\|} \\ \dot{W}_{\alpha\|} \\ \dot{W}_{\alpha\perp} \end{bmatrix} = \int d^3\mathrm{v} \begin{bmatrix} m_\alpha \mathrm{v}_\| \\ m_\alpha \mathrm{v}_\|^2 / 2 \\ m_\alpha \mathrm{v}_\perp^2 / 2 \end{bmatrix} \overline{C}_\alpha \,. \tag{16}$$

The fluid quantities and the anomalous transfer rates are functions s and t and $\overline{C}_\alpha$ is the correlation function for the problem. These equations are general and apply to both upward and downward Birkeland current systems in the Earth's lower magnetosphere from about 1000 km to 2 - 3 Earth radii from the Earth's surface and perhaps beyond. For a review of the work see Jasperse et al. (2006).

In this work, we applied these equations to both downward (DCR) and upward (UCR) current regions when turbulence is included in the calculations and when turbulence is either neglected or is absent in the calculations.

4.1.2 The multiconstituent, multimoment fluid equations in the guiding-center and gyrotropic approximation for weak electromagnetic turbulence.

For weak electromagnetic turbulence, the correlation functions for the wave-particle interactions have a more complicated form than that given in equation (2) for the weak electrostatic turbulence. They are

$$C_\alpha = -\frac{q_\alpha}{m_\alpha} \left\langle \left(\delta\mathbf{E} + \mathbf{v} \times \delta\mathbf{B} \right) . \frac{\partial}{\partial \mathbf{v}} \delta f_\alpha \right\rangle . \tag{17}$$

The multiconstituent, multimoment fluid equations for weak electromagnetic turbulence have the same form as equations (11)-(14) but the expressions for $\dot{M}_{\alpha\|}, \dot{W}_{\alpha\|}$ and $\dot{W}_{\alpha\perp}$ are different than those for weak electrostatic turbulence. They will be discussed in more detail in sections 4.4 and 4.5 of this report.

4.2 Calculations for Downward Birkeland Current Regions.

In this section, we give the steady-state calculations based on FAST satellite data for downward current regions for two cases: (1) when weak electrostatic turbulence is included in the calculation, and (2) when the turbulence is either neglected or absent in the calculation.

4.2.1 Downward current regions (DCRs) when weak electrostatic turbulence is included.

In our work reported in J. Geophys. Res.(2011), we showed calculations when the turbulence was either included or neglected for the two major plasma constituents present in DCRs: a single

up going ion conic and up going field-aligned electrons. In that research effort, we made two approximations: (1) only the up going field-aligned electrons and only one up going ion conic were included, and (2) when the dominant up going ion conic was H^+. FAST and other satellite data show that: a small component of downward propagating plasma sheet ions is also present and the presence of minor constituents of up going O^+ and H_e^+ conics. This gives a total one field-aligned electron component, one precipitating plasma sheet ion component, and three ion conic components, for a total of five plasma constituents.

In this report, we include the presence of downward propagating plasma sheet ions but neglect the minor O^+ and H_e^+ conics. This requires a solution of equations (11) - (15) when a total of three plasma constituents are included.

Table 1. Data for Figures 1 and 2 for a DCR at the FAST Satellite Altitude of 4100 km.

Quantity	Value of Quantity
ion conic density field-aligned electron density plasma sheet ion density	n_{ic} =2.80 (1/cm^3) n_{fae} =3.00 (1/cm^3) n_{psi} =0.20 (1/cm^3)
ion conic velocity field-aligned electron velocity plasma sheet ion velocity	u_{ic} =6.0x10^1 (km/s) u_{fae} =3.5x10^3 (km/s) u_{psi} =1.5x10^2 (km/s)
ion conic $\parallel$ temp. field-aligned electron $\parallel$ temp. plasma sheet ion $\parallel$ temp.	$T_{ic\parallel}$ =5.5x10^1 (ev) $T_{fae\parallel}$ =1.8x10^2 (ev) $T_{psi\parallel}$ =2.0x10^3 (ev)
ion conic$\perp$ temp. field-aligned electron $\perp$ temp. plasma sheet ion$\perp$ temp.	$T_{ic\perp}$ =1.6x10^2 (ev) $T_{fae\perp}$ =1.0 (ev) $T_{psi\perp}$ =3.0x10^3 (ev)

Table 1 shows FAST satellite data from orbit 1678 at the satellite altitude, and Figures 1 and 2 show the steady-state results for weak electrostatic turbulence when the above mentioned three constituents are included.

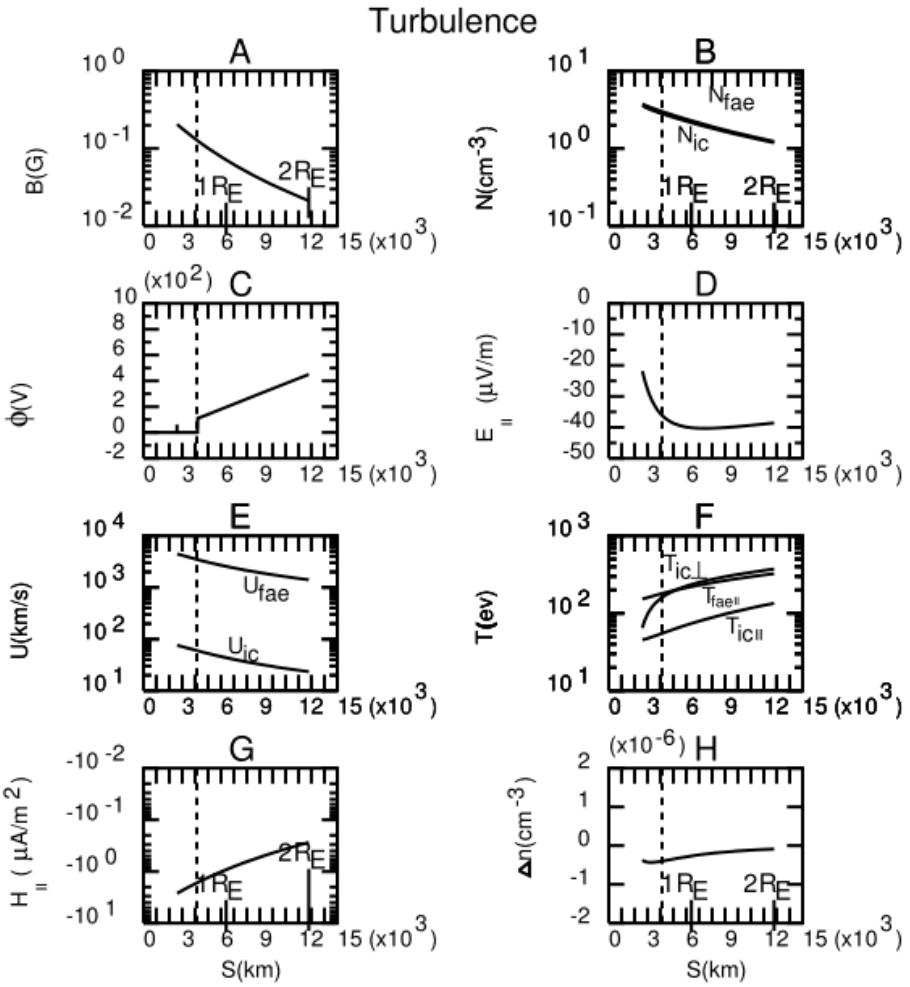

Figure 1. (A-H) The numerical, self-consistent solution for the fluid quantities, ϕ and $E_{\parallel}$ for the quasisteady state for electron bump-on-tail-driven ion cyclotron (EBDIC) turbulence versus s. For a definition of the quantities that appear, see section 4.1.1 and Table 1.

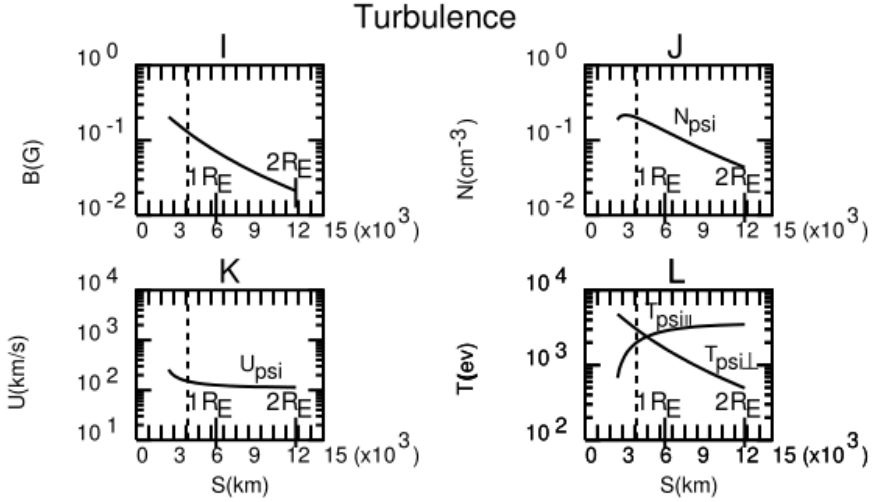

Figure 2. (I-L) Same as Figure 1 but for the plasma sheet ions

Here, compare Figures 1 and 2 to Figure 5 of reference J. Geophys. Res. (2011). We see that the inclusion of a small amount $n_{psi} = (2\times10^{-1}/cm^3)$ of plasma sheet ions makes only a minor difference in the results for the parallel E-field and the electrostatic potential.

In the data shown in Figures 1 and 2, we show a difference by about a factor of three from that reported in J. Geophys. Res. (2011) for u_{fae} . This was obtained by a more accurate determination of the moments from the FAST data. This results in a larger downward current density by about a factor of three from that reported in J. Geophys. Res. (2011). However, comparing Figures 1 and 2 to Figure 1 in J. Geophys. Res. (2011), the other calculated moments are very nearly the same. As mentioned above, the addition of a minor component of plasma sheet ions makes only a small difference in the values for the parallel E-field and the electrostatic potential.

In future work, we plan to make calculations when the minor constituents O^+ and H_e^+ conics are also included. This would require a solution of equations (11) - (15) for the appropriate five constituent plasma.

4.2.2 Downward current regions (DCRs) when weak electrostatic turbulence is neglected or absent.

In J. Geophys. Res. (2011), we also showed calculations for two major plasma constituents (up going field-aligned electrons and an up going H^+ ion conic) when the weak electrostatic turbulence is neglected or absent. Now we show the results for three plasma constituents (up going field-aligned electrons, an up going H^+ conic and down going plasma sheet ions) when the turbulence is neglected or absent. In Table 2, we show the calculated FAST satellite data near the estimated top of the double layer region at an altitude of about 2600 km, and in Figures 3 and 4 we show the steady-state results for the three constituents when the electrostatic turbulence is neglected or absent.

Table 2. Data for Figures 3 and 4 for a DCR at the FAST Satellite Altitude of 2600 km.

Quantity	Value of Quantity
ion conic density field-aligned electron density plasma sheet ion density	n_{ic} =2.80 (1/cm^3) n_{fae} =3.00 (1/cm^3) n_{psi} =0.20 (1/cm^3)
ion conic velocity field-aligned electron velocity plasma sheet ion velocity	u_{ic} =6.00x10^1 (km/s) u_{fae} =3.50x10^3 (km/s) u_{psi} =1.50x10^2 (km/s)
ion conic $\parallel$ temp. field-aligned electron $\parallel$ temp. plasma sheet ion $\parallel$ temp.	$T_{ic\parallel}$ =5.5x10^1 (ev) $T_{fae\parallel}$ =1.8x10^2 (ev) $T_{psi\parallel}$ =2.0x10^3 (ev)
ion conic $\perp$ temp. field-aligned electron $\perp$ temp. plasma sheet ion $\perp$ temp.	$T_{ic\perp}$ =5.5x10^1 (ev) $T_{fae\perp}$ =1.0 (ev) $T_{psi\perp}$ =2.0x10^3 (ev)

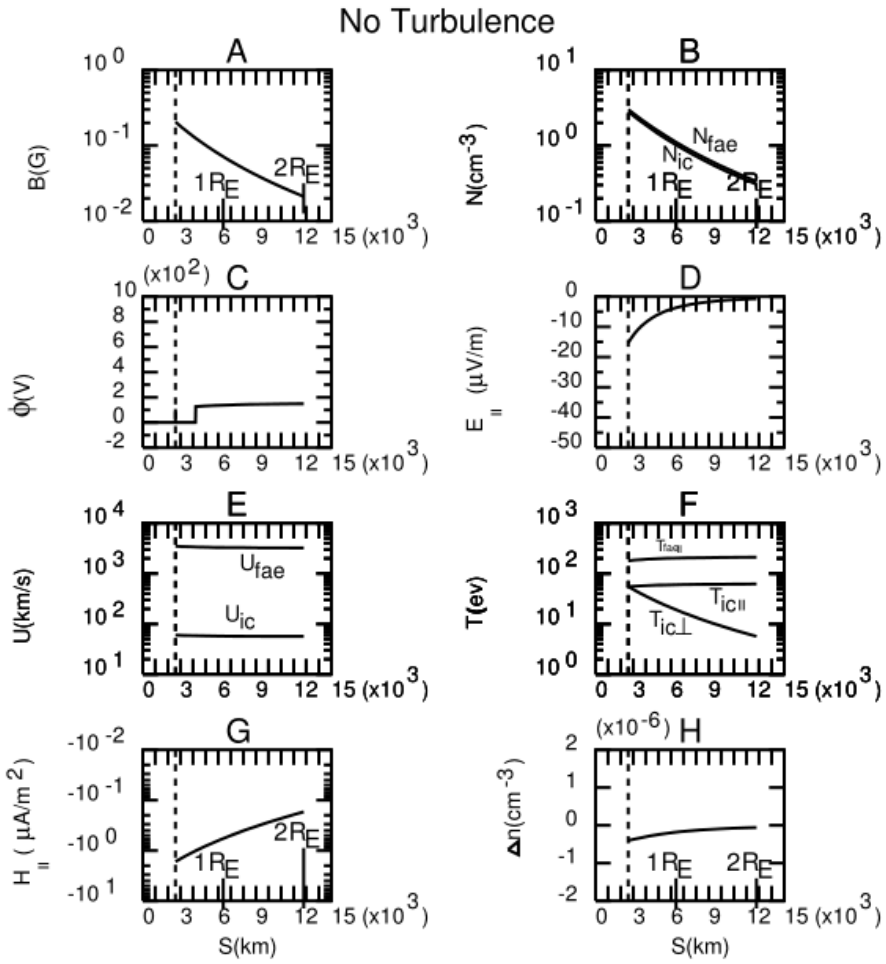

Figure 3. (A-H). The numerical, self-consistent solution for the fluid quantities, ϕ and $E_{||}$ for the quasisteady state when turbulence is neglected or absent. For a definition of the quantities that appear, see section 4.1.1 and Table 2.

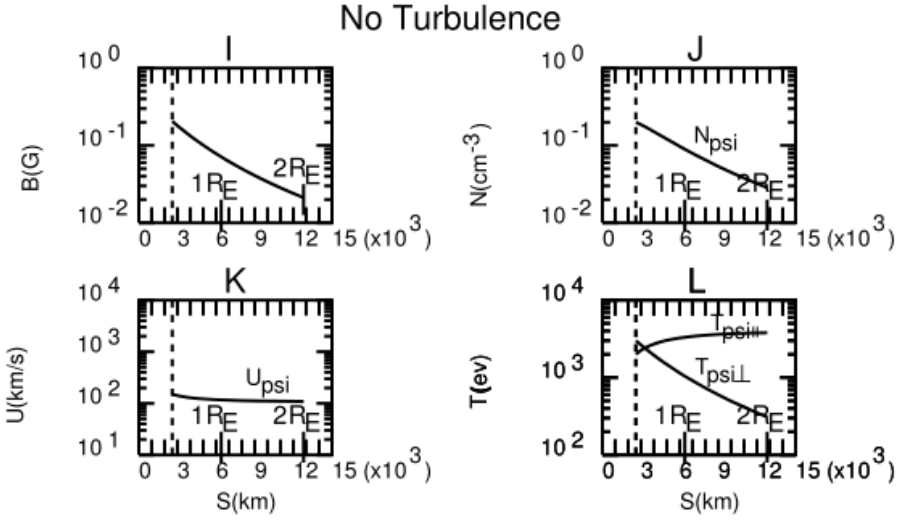

Figure 4. (I-L) Same as Figure 3 but for the plasma sheet ions.

Compare Figures 3 and 4 to Figure 6 in J. Geophys. Res. (2011) for the two dominant plasma constituents.

We see that except for the new values of u_{fae} and $j_{\|}$ from a better determination of the FAST data, the results are very close to those reported in J. Geophys. Res. (2011). Thus, neglecting the presence of the minor component of plasma sheet ions is also a good approximation for $E_{\|}$ and ϕ when the electrostatic turbulence is neglected of absent.

In future calculations, we also plan to include the presence of the minor components of H_e^+ and O^+ ion conics in the calculations for no plasma turbulence.

4.3 Calculations for Upward Birkeland Current Regions.

In McFadden et al. (1999), they discuss upward current regions where auroral density cavities in association with upward ion beams occur. See McFadden et al. (1999), plates 1, 4 and 6, for three examples. In each plate, two regions are shown: (1) the middle of the ion beam region (Plate 1 for the FAST orbit 1616 at a UT of 53.45 seconds) where the ion beam energy flux is about $1\times10^3 eV/cm^2-s-sr-eV$, and (2) the edge of the ion beam region (Plate 1 at a UT of 53.34 seconds) where the ion beam energy flux is reduced to about $40eV/cm^2-s-sr-eV$. For orbit 1616 in Plate 1, note that three plasma constituents occur in the middle of the region but more than three constituents occur at the edge of the region. McFadden et al. (1999) state that three plasma constituents occur in the middle of the region (an upward propagating ion beam, precipitating plasma sheet electrons, and precipitating plasma sheet ions), and at least four constituents occur at the edge of the region (an upward propagating ion beam, precipitating plasma sheet electrons and ions, and a low energy electron population). They also postulate that in the middle of the region, there cannot be any low energy electrons or ions because of the large upward-pointing $E_{\|}$- field; and at the edge of the region , low energy electrons can exist because $E_{\|}$ is very small there. In this report, we solve the appropriate three and four constituent steady-state fluid equations (11) through (15) without turbulence and show that these speculations are correct.

4.3.1 Middle of the upward current region (UCR) when turbulence is neglected.

We did two calculations for the middle of the FAST satellite orbit 1616 at UT= 53.45 seconds. One calculation had no low-energy electrons and the other had a small density ($10^{-4}1/cm^3$) of low- energy electrons.

For the calculation for three constituents (no-low energy electrons) see Table 3 where we show the low-order velocity moments calculated from the satellite orbit 1616 at UT=53.45 seconds at the satellite altitude of 4100 km. Here, we use the following notation: plasma sheet ions (psi), plasma sheet electrons (pse) and ion beam (ib).

Table 3. Data for Figures 5 and 6 in the middle of a URL at the FAST Satellite Altitude of 4100 km.

Quantity	Value of Quantity
plasma sheet ion density plasma sheet electron density ion beam density	n_{psi} =0.80 (1/cm^3) n_{pse} =1.20 (1/cm^3) n_{ib} =0.40 (1/cm^3)
plasma sheet ion velocity plasma sheet electron velocity ion beam velocity	u_{psi} =-6.90x10^2 (km/s) u_{pse} =-1.45x10^4 (km/s) u_{ib} =+3.50x10^2 (km/s)
plasma sheet ion $\parallel$ temp. plasma sheet electron $\parallel$ temp. ion beam $\parallel$ temp.	$T_{psi\parallel}$ =5.0x10^3(ev) $T_{pse\parallel}$ =1.0x10^3(ev) $T_{ib\parallel}$ =1.0x10^2(ev)
plasma sheet ion $\perp$ temp. plasma sheet electron $\perp$ temp. ion beam $\perp$ temp.	$T_{psi\perp}$ =1.5x10^4(ev) $T_{pse\perp}$ =3.0x10^3(ev) $T_{ib\perp}$ =1.0x10^2(ev)

In Figures 5 and 6 we show the calculated steady-state results for the three constituents when turbulence is neglected or absent.

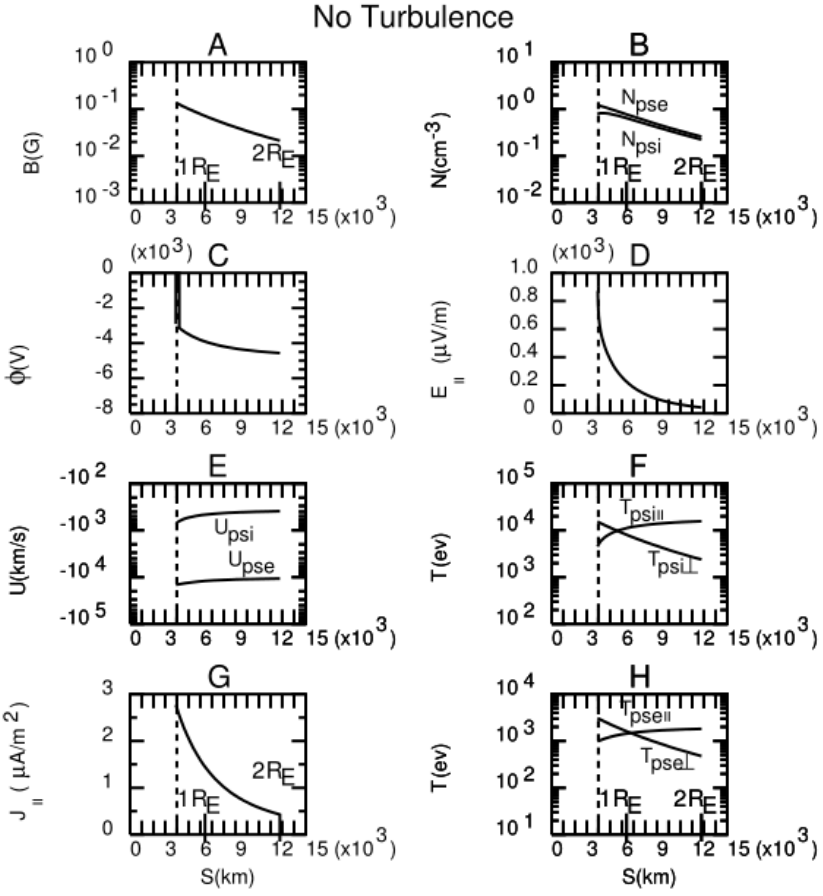

Figure 5. (A-H) The numerical, self-consistent solution for the fluid quantities, ϕ and $E_{||}$ for the quasi-steady state versus s in the middle of a UCR when turbulence is neglected or absent. For a definition of the quantities that appear, see section 4.1.1 and Table 3.

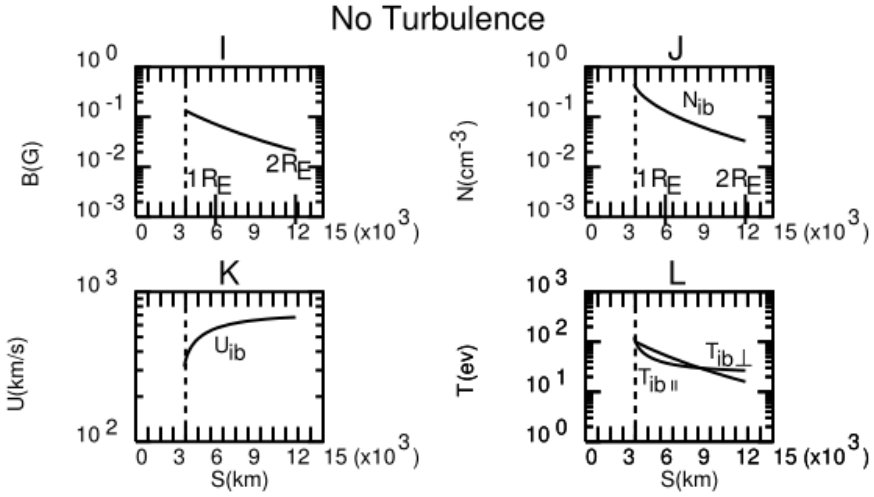

Figure 6. (I-L) Same as Figure 5 but for the ion beam.

Note that using the satellite data and theory, we can estimate a potential drop in the double layer region of about 3 kilovolts. See the J. Geophys. Res. (2011) paper for a discussion on how this estimate is done. We also see that a significant $E_{||}$ and a potential drop of about 1.5 kilovolts occurs above the double layer region even though turbulence has been neglected. This occurs because there can be a significant $E_{||}$-field due to the nonuniform B-field even though the wave-particle interactions have been neglected. See J. Geophys. Rev. (2011) for a discussion of this issue.

When a small amount of low-energy electrons are included as a fourth constituent (with a density $10^{-2}1/cm^{-3}$ or less), we can show that the steady-state multiconstituent, multimoment fluid equations have no solution! The reason for this is that $E_{||}$ repels all the low energy plasma from the region above the double layer region. This result is consistent with the speculation made in McFadden et al. (1999).

We also see the important result that there is a region of space above the satellite altitude from about 4000 km to 8000 km where $T_{ib||} < T_{ib\perp}$ (see Fig. 6). This is very important since in section 4.4 of this report we show that when $T_{ib||} < T_{ib\perp}$ the electromagnetic ion cyclotron waves may be unstable. This condition can drive electromagnetic turbulence, which has been observed by Chaston et al. (1998).

In future work we plan to include electromagnetic turbulence in the calculations. In the upward current region, we speculate that the inclusion of electromagnetic ion cyclotron turbulence will enhance the parallel electric field and the potential drop above the double layer region.

4.3.2 Edge of the upward region (UCR) when turbulence is neglected.

At the edge of the UCR we see from McFadden et al. (1999) data (orbit 1616 at UT=53:34) that there are more than three constituents present. Here we consider four constituents: an upward propagating ion beam, precipitating plasma sheet electrons and plasma sheet ions, and a low-energy electron population. From the data shown in plate 1 at UT= 53:34, we have estimated the low-order moments of the four constituents which are shown in Table 4.

Table 4. Data for Figures 7 and 8 at the edge of a UCR at the FAST Satellite Altitude of 4100 km.

plasma sheet ion density plasma sheet electron density ion beam density low energy electron density	n_{psi} =1.00 (1/cm^3) n_{pse} =2.00 (1/cm^3) n_{ib} =3.00 (1/cm^3) n_{lee} =2.00 (1/cm^3)
plasma sheet ion velocity plasma sheet electron velocity ion beam velocity low energy electron velocity	u_{psi} =-7.0x10^2 (km/s) u_{pse} =-1.5x10^4 (km/s) u_{ib} = 3.5x10^2 (km/s) u_{lee} =-7.0x10^1 (km/s)
plasma sheet ion $\parallel$ temp. plasma sheet electron $\parallel$ temp. ion beam $\parallel$ temp. low energy electron $\parallel$ temp.	$T_{psi\parallel}$ =5.0x10^3(ev) $T_{pse\parallel}$ =1.0x10^3(ev) $T_{ib\parallel}$ =1.0x10^2(ev) $T_{lee\parallel}$ =1.0x10^1(ev)
plasma sheet ion $\perp$ temp. plasma sheet electron $\perp$ temp. ion beam $\perp$ temp. low energy electron $\perp$ temp.	$T_{psi\perp}$ =1.5x10^4(ev) $T_{pse\perp}$ =3.0x10^3(ev) $T_{ib\perp}$ =1.0x10^2(ev) $T_{lee\perp}$ =3.0x10^1(ev)

In Figures 7 and 8, we give the results for the steady-state calculations when the turbulence is neglected or absent.

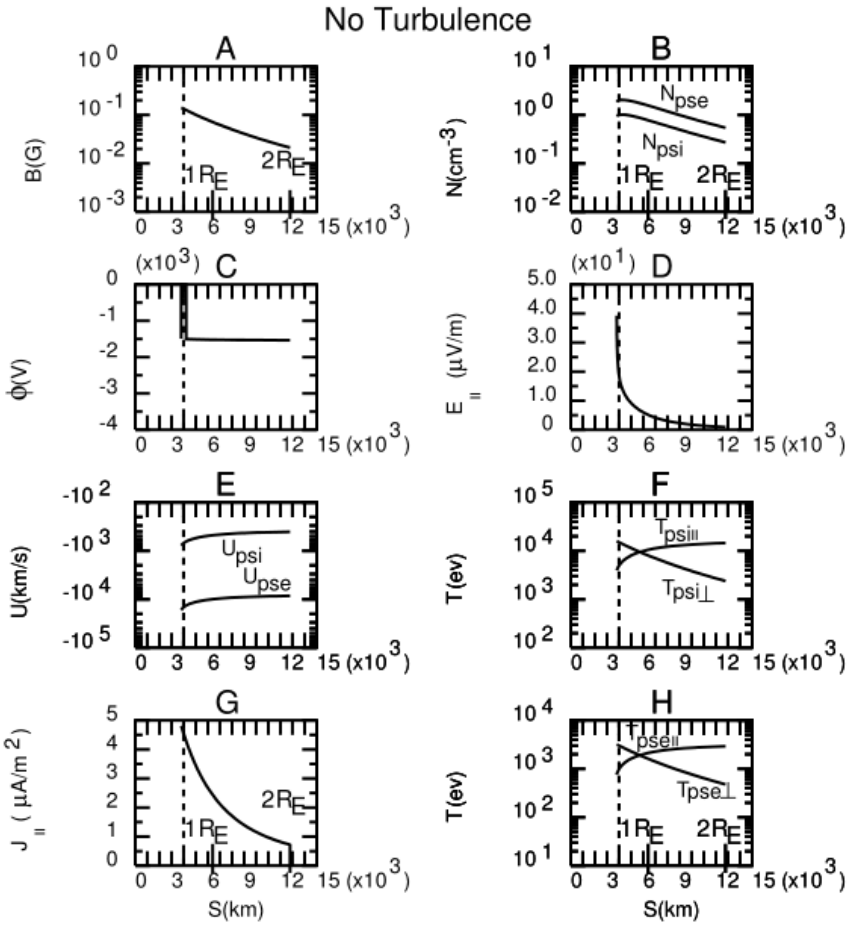

Figure 7. (A-H) The numerical, self-consistent solution for the fluid quantities, ϕ and $E_{\|}$ for the quasi-steady state versus s at the edge of a UCR when the turbulence is neglected or absent. For a definition of the quantities that appear, see section 4.1.1 and Table 4.

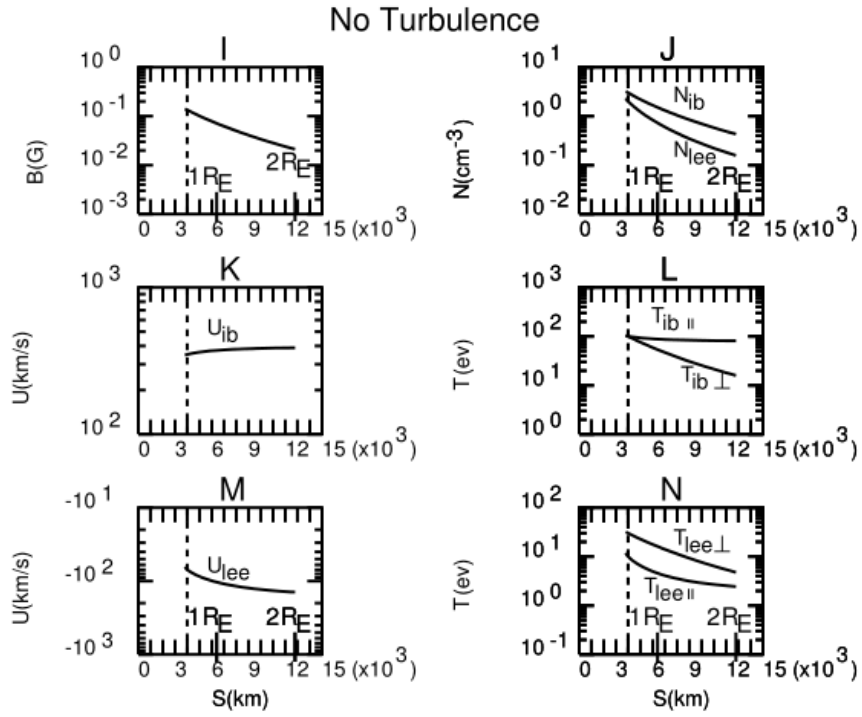

Figure 8. (I-N) Same as Figure 7 but for the ion beam and low-energy electrons.

Several important results are seen here. We see a very small $E_{||}$ (a few $\mu V/m$) above the double layer region and a small potential drop above the double layer region, which is consistent with our assumptions and measurements. We also see that equations (11) – (15) for these four constituents do have a solution. We recall that the multiconstituent, multimoment fluid equations did not have a solution in the middle of the UCR as discussed in section 4.3.1.

In future work we plan to include electromagnetic ion cyclotron turbulence in the calculations. In the middle of the UCR, we speculate that the inclusion of the electromagnetic ion cyclotron turbulence will enhance $E_{||}$ and the potential drop above the double layer region.

4.4 Electromagnetic Ion Cyclotron (EMIC) Waves in the Upward Current Region

We carried out an analytical study of the linear stability properties of obliquely (nearly perpendicular) propagating ($k_\perp / k_{||} > 1$) electromagnetic ion cyclotron (EMIC) waves. Approximate analysis of the linear dispersion relation indicates that a beam-like energetic ion population may excite the fast Alfven waves at the ion cyclotron frequency through cyclotron resonance process and thus may explain the origin of the EMIC waves that have been identified in the upward current region in coincidence with the energetic ion beams [Chaston et al., 1998].

The model that we consider is a three component plasma consisting of electrons, thermal ions and energetic ions, denoted by the subscripts e, i, and ib, respectively. We then consider the so-called extraordinary electromagnetic waves in the ambient plasma that, in the absence of the energetic ions, propagate in the $x-z$ plane while the ambient magnetic field $\mathbf{B}_0$ is along the

z - axis. That is, $\mathbf{k} = (k_\perp, 0, k_\parallel)$ and $\mathbf{B}_0 = (0,0,B_0)$. The wave electric field $\delta\tilde{\mathbf{E}}$ is taken to be in the $x-y$ plane, and the wave magnetic field $\delta\tilde{\mathbf{B}}$ is given by $\mathbf{k}\times\delta\tilde{\mathbf{E}} = (\omega/c)\delta\tilde{\mathbf{B}}$ for perturbations of the form: $\exp(i\mathbf{k}\cdot\mathbf{r} - i\omega t)$. It then follows from the Maxwell equations that the considered electromagnetic waves must satisfy the dispersion relation

$$\left(\frac{c^2k_\parallel^2}{\omega^2} - \varepsilon_{xx}\right)\left(\frac{c^2k^2}{\omega^2} - \varepsilon_{yy}\right) = \varepsilon_{xy}\varepsilon_{yx}, \tag{18}$$

where $k^2 \equiv k_\parallel^2 + k_\perp^2$ and ε_{ij} are the elements of the dielectric tensor $\boldsymbol{\varepsilon}$.

The theoretical approach is to solve the linearized Vlasov equation to find the perturbed distribution function $\tilde{f}_\alpha(\mathbf{k},\mathbf{v},\omega)$, which is used to calculate the perturbed current density $\tilde{\mathbf{j}}(\mathbf{k},\omega)$. From the perturbed current density the elements of the conductivity tensor $\boldsymbol{\sigma}(\mathbf{k},\omega)$ and then the elements of the dielectric tensor $\boldsymbol{\varepsilon}(\mathbf{k},\omega)$ are determined from the relation $\boldsymbol{\varepsilon} = \mathbf{I} + (4\pi i/\omega)\boldsymbol{\sigma}$. Solving the linearized Vlasov equation by the standard procedure, the relevant components of the perturbed current density $\tilde{\mathbf{j}}(\mathbf{k},\omega)$ are obtained as

$$\tilde{j}_x = -i\sum_\alpha \frac{2\pi q_\alpha^2}{m_\alpha}\sum_{n=-\infty}^{+\infty}\int d\mathrm{v}_\parallel d\mathrm{v}_\perp \frac{\mathrm{v}_\perp^2}{\omega - k_\parallel \mathrm{v}_\parallel - n\Omega_\alpha}\frac{n}{\mu_\alpha}J_n(\mu_\alpha)\tilde{G}_{\alpha n}, \tag{19}$$

$$\tilde{j}_y = -\sum_\alpha \frac{2\pi q_\alpha^2}{m_\alpha}\sum_{n=-\infty}^{+\infty}\int d\mathrm{v}_\parallel d\mathrm{v}_\perp \frac{\mathrm{v}_\perp^2}{\omega - k_\parallel \mathrm{v}_\parallel - n\Omega_\alpha}J_n'(\mu_\alpha)\tilde{G}_{\alpha n}, \tag{20}$$

where

$$\tilde{G}_{\alpha n} \equiv \left[\frac{n}{\mu_\alpha}J_n(\mu_\alpha)\delta\tilde{E}_x + iJ_n'(\mu_\alpha)\delta\tilde{E}_y\right]\left[\frac{\partial}{\partial \mathrm{v}_\perp} - \frac{k_\parallel}{\omega}\left(\mathrm{v}_\parallel\frac{\partial}{\partial \mathrm{v}_\perp} - \mathrm{v}_\perp\frac{\partial}{\partial \mathrm{v}_\parallel}\right)\right]F_\alpha, \tag{21}$$

$\mu_\alpha \equiv k_\perp \mathrm{v}_\perp/\Omega_\alpha$, $J_n'(\mu_\alpha) \equiv dJ_n/d\mu_\alpha$, and F_α is the unperturbed particle distribution function.

We first study the dispersion relation for EMIC waves in the absence of the energetic ion population. For this we assume, for illustration purposes, that the unperturbed distribution functions of the thermal electrons and ions can be modelled by Maxwellians with anisotropic temperatures and are given by

$$F_\alpha = \left(\frac{m_\alpha}{2\pi}\right)^{3/2}\frac{n_\alpha}{T_{\alpha\perp}T_{\alpha\parallel}^{1/2}}\exp\left(-\frac{m_\alpha \mathrm{v}_\perp^2}{2T_{\alpha\perp}} - \frac{m_\alpha \mathrm{v}_\parallel^2}{2T_{\alpha\parallel}}\right), \tag{22}$$

where $\alpha = e, i$. Then, the elements of the dielectric tensor $\boldsymbol{\varepsilon}$ are

$$\varepsilon_{xx} = 1 - \sum_{\alpha} \frac{\omega_{p\alpha}^2}{\omega^2} \sum_{n=-\infty}^{+\infty} \frac{n^2}{\xi_\alpha} \Gamma_n(\xi_\alpha) \left\{ \frac{\omega}{\omega - n\Omega_\alpha} \left[1 + W(\zeta_{\alpha n})\right] - \left(1 - \frac{T_{\alpha\perp}}{T_{\alpha\parallel}}\right) W(\zeta_{\alpha n}) \right\}, \quad (23)$$

$$\varepsilon_{xy} = -\varepsilon_{yx} = -i \sum_{\alpha} \frac{\omega_{p\alpha}^2}{\omega^2} \sum_{n=-\infty}^{+\infty} n\Gamma_n'(\xi_\alpha) \left\{ \frac{\omega}{\omega - n\Omega_\alpha} \left[1 + W(\zeta_{\alpha n})\right] - \left(1 - \frac{T_{\alpha\perp}}{T_{\alpha\parallel}}\right) W(\zeta_{\alpha n}) \right\}, \quad (24)$$

$$\varepsilon_{yy} = 1 - \sum_{\alpha} \frac{\omega_{p\alpha}^2}{\omega^2} \sum_{n=-\infty}^{+\infty} \left[\frac{n^2}{\xi_\alpha} \Gamma_n(\xi_\alpha) - 2\xi_\alpha \Gamma_n'(\xi_\alpha) \right] \left\{ \frac{\omega}{\omega - n\Omega_\alpha} \left[1 + W(\zeta_{\alpha n})\right] - \left(1 - \frac{T_{\alpha\perp}}{T_{\alpha\parallel}}\right) W(\zeta_{\alpha n}) \right\}. \quad (25)$$

Here, $\omega_{p\alpha}^2 \equiv 4\pi q_\alpha^2 n_\alpha / m_\alpha$, $\Omega_\alpha \equiv q_\alpha B_0 / (m_\alpha c)$, $\Gamma_n(\xi_\alpha) \equiv I_n(\xi_\alpha)\exp(-\xi_\alpha)$, $\xi_\alpha \equiv k_\perp^2 T_{\alpha\perp} / (m_\alpha \Omega_\alpha^2)$, $\Gamma_n'(\xi_\alpha) \equiv d\Gamma_n / d\xi_\alpha$, I_n is the modified Bessel function, and $W(\zeta_{\alpha n}) \equiv -1 - \zeta_{\alpha n} Z(\zeta_{\alpha n})$, where $\zeta_{\alpha n} \equiv (\omega - n\Omega_\alpha)/(k_\parallel V_{T\alpha\parallel})$, $V_{T\alpha\parallel}^2 \equiv 2T_{\alpha\parallel} / m_\alpha$, and $Z(\zeta_{\alpha n})$ is the well-known plasma dispersion function. We simplify the analysis by considering $\xi_\alpha << 1$, whereby the expressions for ε_{ij} become

$$\varepsilon_{xx} = \varepsilon_{yy}$$
$$\cong 1 - \sum_{\alpha} \frac{\omega_{p\alpha}^2}{\omega^2 - \Omega_\alpha^2} - \sum_{\alpha} \frac{\omega_{p\alpha}^2}{2\omega^2} \left\{ \left[\frac{\omega}{\omega - \Omega_\alpha} - \left(1 - \frac{T_{\alpha\perp}}{T_{\alpha\parallel}}\right) \right] W_- + \left[\frac{\omega}{\omega + \Omega_\alpha} - \left(1 - \frac{T_{\alpha\perp}}{T_{\alpha\parallel}}\right) \right] W_+ \right\}, \quad (26)$$

$$\varepsilon_{xy} = -\varepsilon_{yx}$$
$$\cong -i \sum_{\alpha} \frac{\omega_{p\alpha}^2 \Omega_\alpha}{\omega(\omega^2 - \Omega_\alpha^2)} - i \sum_{\alpha} \frac{\omega_{p\alpha}^2}{2\omega^2} \left\{ \left[\frac{\omega}{\omega - \Omega_\alpha} - \left(1 - \frac{T_{\alpha\perp}}{T_{\alpha\parallel}}\right) \right] W_- - \left[\frac{\omega}{\omega + \Omega_\alpha} - \left(1 - \frac{T_{\alpha\perp}}{T_{\alpha\parallel}}\right) \right] W_+ \right\}. \quad (27)$$

Here $W_\pm$ refers to its argument $\zeta_{\alpha\pm} \equiv (\omega \pm \Omega_\alpha)/(k_\parallel V_{T\alpha\parallel})$. The dispersion relation [Eq. (18)] with the substitution of the results given in Eqs. (26) and (27) describes electromagnetic waves on the fast Alfven and ion Bernstein wave branches. Here we are interested in the fast Alfven wave branch, for which the expressions for ε_{ij} can be further simplified by considering $|\omega/\Omega_\alpha| < 1$ and $|k_\parallel V_{T\alpha\parallel} / \Omega_\alpha| < 1$. The results are

$$\varepsilon_{xx} = \varepsilon_{yy} \cong 1 + \frac{c^2}{V_A^2} + \sum_{\alpha} \frac{\omega_{p\alpha}^2}{\omega^2} \left\{ \left(1 - \frac{T_{\alpha\perp}}{T_{\alpha\parallel}}\right) \frac{k_\parallel^2 T_{\alpha\parallel}}{m_\alpha \Omega_\alpha^2} + i\sqrt{\pi} \frac{T_{\alpha\perp}}{T_{\alpha\parallel}} \frac{\omega}{|k_\parallel| V_{T\alpha\parallel}} \exp\left(-\frac{\Omega_\alpha^2}{k_\parallel^2 V_{T\alpha\parallel}^2} \right) \right\}, \quad (28)$$

$$\varepsilon_{xy} = -\varepsilon_{yx} \cong i \sum_{\alpha} \frac{\omega_{p\alpha}^2}{\omega^2} \left(1 - \frac{T_{\alpha\perp}}{T_{\alpha\parallel}}\right) \left\{ \frac{2k_\parallel^2 T_{\alpha\parallel}}{m_\alpha \Omega_\alpha^2} \frac{\omega}{\Omega_\alpha} + i\sqrt{\pi} \frac{T_{\alpha\perp}}{T_{\alpha\parallel}} \frac{\Omega_\alpha}{|k_\parallel| V_{T\alpha\parallel}} \exp\left(-\frac{\Omega_\alpha^2}{k_\parallel^2 V_{T\alpha\parallel}^2} \right) \right\}. \quad (29)$$

where V_A is the Alfven speed. Then, the low frequency ($\omega << ck$) solution of the dispersion relation [Eq. (18)] is obtained as

$$\frac{\omega}{kV_A} \cong 1 - \frac{1}{4}\sum_{\alpha}\frac{\omega_{p\alpha}^2}{c^2k^2}\left(1-\frac{T_{\alpha\perp}}{T_{\alpha\|}}\right)\frac{k_\|^2 V_{T\alpha\|}^2}{\Omega_\alpha^2} - i\frac{\sqrt{\pi}}{2}\sum_{\alpha}\frac{\omega_{p\alpha}^2}{c^2 k|k_\||}\frac{V_A}{V_{T\alpha\|}}\frac{T_{\alpha\perp}}{T_{\alpha\|}}\exp\left(-\frac{\Omega_\alpha^2}{k_\|^2 V_{T\alpha\|}^2}\right). \quad (30)$$

In the limit, $k_\| \to 0$, Eq. (30) gives $\omega \cong kV_A$, which are the fast Alfven waves. Finite-$k_\|$ adds a small correction to $\mathrm{Re}\,\omega$ for low-β plasmas, while the imaginary term represents the transit-time damping rate (due to wave-particle resonance with the thermal electrons and the thermal ions), which is the magnetic analog of Landau damping rate and which is also small for low-β plasmas. It is evident that the $\alpha = i$ term is the dominant term in the damping rate.

Next, we add the relevant contribution of the energetic ion population to Eq. (30). For this, we model the energetic ion population with unperturbed distribution function given by

$$F_{ib} = \left(\frac{m_{ib}}{2\pi}\right)^{3/2}\frac{n_{ib}}{T_{ib\perp}T_{ib\|}^{1/2}}\exp\left[-\frac{m_{ib}}{2T_{ib\perp}}\mathrm{v}_\perp^2 - \frac{m_{ib}}{2T_{ib\|}}\left(\mathrm{v}_\| - u_{ib}\right)^2\right], \quad (31)$$

and considering the cyclotron resonance condition

$$\omega - k_\|\mathrm{v}_\| - \Omega_b = 0, \quad (32)$$

where Ω_b is the beam ion cyclotron frequency, we find that Eq. (30) is modified as

$$\frac{\omega}{kV_A} \cong [\text{RHS of Eq. (30)}] + i\frac{\sqrt{\pi}}{4}\frac{\omega_{pb}^2}{c^2k^2}\frac{T_{ib\perp}}{T_{ib\|}}\frac{1}{|k_\||V_{Tb\|}}\left[\left(1-\frac{T_{ib\|}}{T_{ib\perp}}\right)\Omega_b - \bar{\omega}\right]. \quad (33)$$

for $\xi_b \equiv k_\perp^2 T_{ib\perp}/(m_{ib}\Omega_b^2) << 1$ and $\left|(\bar{\omega}-\Omega_b)/(k_\|V_{Tb\|})\right| < 1$. Here $\omega_{pb}^2 \equiv 4\pi q_{ib}^2 n_{ib}/m_{ib}$, $V_{Tb\|}^2 \equiv 2T_{ib\|}/m_{ib}$, and $\bar{\omega} \equiv \omega - k_\| u_{ib}$. This indicates that, in order to excite the instability (i.e., $\mathrm{Im}\,\omega > 0$), (1) the condition given by

$$\bar{\omega} < \left(1-\frac{T_{ib\|}}{T_{ib\perp}}\right)\Omega_b, \quad (34)$$

has to be satisfied and, in addition, (2) the positive imaginary term in Eq. (33) due to the streaming ion population has to overcome the negative imaginary terms (damping terms) in Eq. (30). The condition given by Eq. (34) suggests that a streaming ion distribution with less thermal spread in the parallel direction ($T_{ib\|} < T_{ib\perp}$), i.e., a more beam-like ion distribution is required for the onset of the instability.

Clearly, the conditions for the excitation of the instability depend on $|k_\||$, $k_\perp$, and the various plasma and beam parameters appearing in Eqs. (30), (33) and (34). Numerical estimates, based on the plasma and beam parameters given in Table 3, while taking $B_0 \cong 0.1$ G, show that for appropriate choices of $|k_\||$, $k_\perp$ that are consistent with the assumptions made in the above

analysis all the conditions for instability can be satisfied when $T_{ib\|} < T_{ib\perp}$. This may account for the origin of the electromagnetic turbulence, which has been observed by Chaston et al. (1998), as our theoretical calculations show that there is a region of space above the satellite altitude from about 4000 km to 8000 km where $T_{ib\|} < T_{ib\perp}$ (see Fig. 6). However, we should add that this conclusion is based on the approximate analysis of the dispersion relation. A rigorous numerical analysis of the dispersion relation, with the expressions for the elements of the dielectric tensor given by Eq. (23) – (25), has to be carried out for a more accurate theoretical prediction. Moreover, in order to verify the theoretical predictions, measurements of the spectral information $(k_{\|}, k_{\perp})$ about the observed EMIC waves are necessary. The EMIC turbulence is expected to increase $T_{ib\|} / T_{ib\perp}$ from its initial value of less than unity (required for the excitation of the instability) to a value ~1 when the instability will be quenched. Hence, we may speculate that EMIC turbulence could be observed even if satellite measurements indicate $T_{ib\|} \sim T_{ib\perp}$, as satellite measurements may possibly have been made in a fully developed turbulent state.

4.5 Calculation of Anomalous Momentum and Energy Transfer Rates in the Presence of EMIC Turbulence

In order to calculate the anomalous momentum and energy transfer rates $(\dot{M}_{\alpha\|}, \dot{W}_{\alpha\|}, \dot{W}_{\alpha\perp})$ due to wave-particle interactions in the presence of the electromagnetic turbulence generated by the above-mentioned instability, we need to extend the formalisms of Ichimaru and Rosenbluth [1970], as adopted by Jasperse et al. [2006], by including the additional effects of magnetic field fluctuations. It is a rather formidable task. An alternative procedure adopted by Matsuda [1983], including the effects of only electrostatic fluctuations, shows that the resultant kinetic equation reduces to the well-known quasilinear diffusion equation of the weak turbulence theory if the effects of the self-field of the charged particles are ignored. Thus, for mathematical simplicity, we opted to use the quasilinear diffusion equation in the presence of electromagnetic turbulence and calculated the anomalous momentum and energy transfer rates $(\dot{M}_{\alpha\|}, \dot{W}_{\alpha\|}, \dot{W}_{\alpha\perp})$ due to resonant wave-particle interactions.

4.5.1 Quasilinear equation for electromagnetic wave-particle interactions

Following the standard formalism of the weak-turbulence theory, we obtain the following kinetic equation that describes both resonant and non-resonant wave-particle interactions in the presence of the considered extraordinary electromagnetic turbulence.

$$\begin{aligned}\frac{\partial F_\alpha}{\partial t} \cong\, & i\frac{q_\alpha^2}{m_\alpha^2}\int d\mathbf{k}\left|\delta\tilde{E}_x(\mathbf{k},t)\right|^2\left[\left(1-\frac{k_\parallel \mathrm{v}_\parallel}{\omega_k}\right)\left(\frac{\partial}{\partial \mathrm{v}_\perp}+\frac{1}{\mathrm{v}_\perp}\right)+\frac{k_\parallel \mathrm{v}_\perp}{\omega_k}\frac{\partial}{\partial \mathrm{v}_\parallel}\right] \\ & \times\left\{\sum_{n=-\infty}^{+\infty}\frac{n^2}{\mu_\alpha^2}\frac{J_n^2(\mu_\alpha)}{\omega_k-k_\parallel \mathrm{v}_\parallel-n\Omega_\alpha}\left[\left(1-\frac{k_\parallel \mathrm{v}_\parallel}{\omega_k}\right)\frac{\partial}{\partial \mathrm{v}_\perp}+\frac{k_\parallel \mathrm{v}_\perp}{\omega_k}\frac{\partial}{\partial \mathrm{v}_\parallel}\right]F_\alpha\right\} \\ & + i\frac{q_\alpha^2}{m_\alpha^2}\int d\mathbf{k}\left|\delta\tilde{B}_z(\mathbf{k},t)\right|^2\frac{\omega_k^2}{c^2k^2}\left[\left(1-\frac{k_\parallel \mathrm{v}_\parallel}{\omega_k}\right)\left(\frac{\partial}{\partial \mathrm{v}_\perp}+\frac{1}{\mathrm{v}_\perp}\right)+\frac{k_\parallel \mathrm{v}_\perp}{\omega_k}\frac{\partial}{\partial \mathrm{v}_\parallel}\right] \\ & \times\left\{\sum_{n=-\infty}^{+\infty}\frac{J_n'^2(\mu_\alpha)}{\omega_k-k_\parallel \mathrm{v}_\parallel-n\Omega_\alpha}\left[\left(1-\frac{k_\parallel \mathrm{v}_\parallel}{\omega_k}\right)\frac{\partial}{\partial \mathrm{v}_\perp}+\frac{k_\parallel \mathrm{v}_\perp}{\omega_k}\frac{\partial}{\partial \mathrm{v}_\parallel}\right]F_\alpha\right\}\end{aligned} \tag{35}$$

In obtaining Eq. (35), we have used $\delta\tilde{E}_y(\mathbf{k},t)=(\omega_k/ck_\perp)\delta\tilde{B}_z(\mathbf{k},t)$ and have made the assumption that the field fluctuations are excited in an axisymmetric manner, corresponding to

$$\left\langle\left|\delta\tilde{E}_x(\mathbf{k},t)\right|^2\right\rangle=\left\langle\left|\delta\tilde{E}_y(\mathbf{k},t)\right|^2\right\rangle,\quad \left\langle\delta\tilde{E}_x^*(\mathbf{k},t)\delta\tilde{E}_y(\mathbf{k},t)\right\rangle=\left\langle\delta\tilde{E}_y^*(\mathbf{k},t)\delta\tilde{E}_x(\mathbf{k},t)\right\rangle=0. \tag{36}$$

4.5.2 Expressions for $\dot{M}_{\alpha\parallel}, \dot{W}_{\alpha\parallel}$, and $\dot{W}_{\alpha\perp}$ due to resonant wave-particle interactions

In calculating $\dot{M}_{\alpha\parallel}, \dot{W}_{\alpha\parallel}$, and $\dot{W}_{\alpha\perp}$, according to the definitions given by Eq. (16) where $\partial F_\alpha/\partial t$ is given by Eq, (35), we use, as an approximation, initial Maxwellian distributions for F_α on the right-hand side of Eq. (35). This allows us to evaluate all the velocity space integrals in closed form, while the significant leading order effects of turbulence are taken into account. Considering only the resonant wave-particle interactions we find

$$\begin{aligned}\dot{M}_{\alpha\parallel} \cong\, & \frac{\omega_{p\alpha}^2}{4}\left(\frac{m_\alpha}{2\pi T_{\alpha\parallel}}\right)^{1/2}\frac{T_{\alpha\perp}}{T_{\alpha\parallel}}\sum_{n=-\infty}^{+\infty}\int d\mathbf{k}\left\{\frac{\left|\delta\tilde{E}_x(\mathbf{k},t)\right|^2}{\omega_k^2}\frac{n^2}{\xi_\alpha}\Gamma_n(\xi_\alpha)+\frac{\left|\delta\tilde{B}_z(\mathbf{k},t)\right|^2}{c^2k_\perp^2}\right. \\ & \left.\times\left[\frac{n^2}{\xi_\alpha}\Gamma_n(\xi_\alpha)-2\xi_\alpha\Gamma_n'(\xi_\alpha)\right]\right\}\left[\omega_k-n\Omega_\alpha\left(1-\frac{T_{\alpha\parallel}}{T_{\alpha\perp}}\right)\right]\exp\left[-\frac{m_\alpha}{2T_{\alpha\parallel}}\left(\frac{\omega_k-n\Omega_\alpha}{k_\parallel}\right)^2\right],\end{aligned} \tag{37}$$

$$\begin{aligned}\dot{W}_{\alpha\parallel} \cong\, & \frac{\omega_{p\alpha}^2}{4}\left(\frac{m_\alpha}{2\pi T_{\alpha\parallel}}\right)^{1/2}\frac{T_{\alpha\perp}}{T_{\alpha\parallel}}\sum_{n=-\infty}^{+\infty}\int d\mathbf{k}\,\frac{\omega_k-n\Omega_\alpha}{k_\parallel}\left\{\frac{\left|\delta\tilde{E}_x(\mathbf{k},t)\right|^2}{\omega_k^2}\frac{n^2}{\xi_\alpha}\Gamma_n(\xi_\alpha)+\frac{\left|\delta\tilde{B}_z(\mathbf{k},t)\right|^2}{c^2k_\perp^2}\right. \\ & \left.\times\left[\frac{n^2}{\xi_\alpha}\Gamma_n(\xi_\alpha)-2\xi_\alpha\Gamma_n'(\xi_\alpha)\right]\right\}\left[\omega_k-n\Omega_\alpha\left(1-\frac{T_{\alpha\parallel}}{T_{\alpha\perp}}\right)\right]\exp\left[-\frac{m_\alpha}{2T_{\alpha\parallel}}\left(\frac{\omega_k-n\Omega_\alpha}{k_\parallel}\right)^2\right],\end{aligned} \tag{38}$$

and

$$\dot{W}_{\alpha\perp} \cong \frac{\omega_{p\alpha}^2}{4}\left(\frac{m_\alpha}{2\pi T_{\alpha\|}}\right)^{1/2}\frac{T_{\alpha\perp}}{T_{\alpha\|}}\sum_{n=-\infty}^{+\infty}\int d\mathbf{k}\,\frac{n\Omega_\alpha}{k_\|}\left\{\frac{\left|\delta\tilde{E}_x(\mathbf{k},t)\right|^2}{\omega_k^2}\frac{n^2}{\xi_\alpha}\Gamma_n(\xi_\alpha)+\frac{\left|\delta\tilde{B}_z(\mathbf{k},t)\right|^2}{c^2k_\perp^2}\right.$$
$$\left.\times\left[\frac{n^2}{\xi_\alpha}\Gamma_n(\xi_\alpha)-2\xi_\alpha\Gamma'_n(\xi_\alpha)\right]\right\}\left[\omega_k-n\Omega_\alpha\left(1-\frac{T_{\alpha\|}}{T_{\alpha\perp}}\right)\right]\exp\left[-\frac{m_\alpha}{2T_{\alpha\|}}\left(\frac{\omega_k-n\Omega_\alpha}{k_\|}\right)^2\right]. \quad (39)$$

We recall that $\omega_{p\alpha}^2 \equiv 4\pi q_\alpha^2 n_\alpha / m_\alpha$, $\Omega_\alpha \equiv q_\alpha B_0/(m_\alpha c)$, $\Gamma_n(\xi_\alpha) \equiv I_n(\xi_\alpha)\exp(-\xi_\alpha)$, $\Gamma'_n(\xi_\alpha) \equiv d\Gamma_n / d\xi_\alpha$, where $\xi_\alpha \equiv k_\perp^2 T_{\alpha\perp}/(m_\alpha\Omega_\alpha^2)$ and I_n is the modified Bessel function. For application to the EMIC instability described in Section 4.4, the expressions can be simplified as $\xi_\alpha << 1$.

4.6 References

Chaston, C. C., R. E. Ergun, G. T. Delory, W. Peria, M. Temerin, C. Catell, R. Strangeway, J. P. McFadden, C. W. Carlson, R. C. Elphic, D. M. Klumpar, W. K. Peterson, E. Mobius, and R. Pfaff (1998), Characteristics of electromagnetic proton cyclotron waves along auroral field lines observed by FAST in regions of upward current, *Geophys. Res. Lett*. **25**, 2057.

Ichimaru, S. and M. N. Rosenbluth (1970), Relaxation processes in plasmas with magnetic field. Temperature relaxations, *Phys. Fluids* **13**, 2778.

Jasperse, J. R., B. Basu, E. J. Lund, and M. Bouhram (2006), Gyrotropic guiding-center fluid theory for turbulent inhomogeneous magnetized plasma, *Phys. Plasmas* **13**, 072903.

Jasperse, J. R., B. Basu, E. J. Lund, and N. Grossbard (2011), Anomalous transport effects on the parallel E field in downward auroral current regions of the Earth's magnetosphere, *J. Geophys. Res.*, A00K11.

Matsuda, K (1983), Fokker-Planck equation for a plasma in a magnetic field with electrostatic fluctuations, *Phys. Fluids* **26**, 1508.

McFadden, J. P., C. W. Carlson, R. E. Ergun, D. M. Klumpar, and E. Moebius (1999), Ion and electron characteristics in auroral density cavities associated with ion beams: No evidence for cold ionospheric plasma, *J. Geophys. Res.* **104**, 14,671.

5. Personnel Supported

Dr. John Jasperse, Boston College.

Dr. Bamandas Basu, Boston College.

Mr. Neil Grossbard, Boston College.

Dr. John Retterer, Boston College.

6. Publications

Coppi, B., B. Basu, and A. Fletcher (2017), Magneto-thermal reconnection processes, related mode momentum and formation of high energy particle populations, *Nucl. Fusion*, **57**, 076028.

Coppi, B and B. Basu, Endogenous magnetic reconnection and associated high energy plasma processes, *Phys. Lett. A*, **382**, 400, 2018.

Jasperse, J. R., B. Basu, J. Retterer, and N. Grossbard (2019), Transport effects in upward and downward auroral current systems in the Earth's magnetosphere, to be submitted to *J. Geophys. Res.*

7. Scientific Visitors

Dr. Mahboubeh Asgari-Targhi, Center for Astrophysics, Harvard University.

Dr. Alex Fletcher, Center for Space Physics, Boston University.

Dr. Mikhail V. Medvedev, Center for Astrophysics, Harvard University.

8. Collaborative Research Projects

"Pitch-angle scattering and formation of high energy particle populations during magnetic reconnection events", with B. Coppi (MIT) and A. Fletcher (Boston University).

9. Technology Transitions

We have developed and made available to the research community four computer codes: two codes for DCRs including the effect plasma sheet ions with and without electrostatic ion cyclotron turbulence; and two codes for UCRs without turbulence (one when three constituents are present and the other when four constituents are present).